②

DISC-E-95GP-0301

DIRECTORATE OF ENGINEERING & STANDARDIZATION

REPORT OF FINDINGS: ENGINEERING PRACTICES STUDY ON FAILURE ANALYSIS OF
NSN 5340-00-136-9872 GROOVED COUPLING CLAMP

AD-A204 710

Bohdan Hasiuk
Defense Industrial Supply Center
DISC-ECM
700 Robbins Avenue
Philadelphia, PA 19111-5096

3 October 1988

DTIC
SELECTED
0 3 JAN 1989
E

DEFENSE INDUSTRIAL SUPPLY CENTER

89   1 03 011

REPORT DOCUMENTATION PAGE

1a. REPORT SECURITY CLASSIFICATION	1b. RESTRICTIVE MARKINGS
Unclassified	

2a. SECURITY CLASSIFICATION AUTHORITY	3. DISTRIBUTION / AVAILABILITY OF REPORT
2b. DECLASSIFICATION / DOWNGRADING SCHEDULE	

4. PERFORMING ORGANIZATION REPORT NUMBER(S)	5. MONITORING ORGANIZATION REPORT NUMBER(S)
DISC-E-95GP-0301	

6a. NAME OF PERFORMING ORGANIZATION	6b. OFFICE SYMBOL (If applicable)	7a. NAME OF MONITORING ORGANIZATION
Defense Industrial Supply Center	DISC-ECM	

6c. ADDRESS (City, State, and ZIP Code)	7b. ADDRESS (City, State, and ZIP Code)
Philadelphia, PA 19111-5096	

8a. NAME OF FUNDING / SPONSORING ORGANIZATION	8b. OFFICE SYMBOL (If applicable)	9. PROCUREMENT INSTRUMENT IDENTIFICATION NUMBER

8c. ADDRESS (City, State, and ZIP Code)	10. SOURCE OF FUNDING NUMBERS			
	PROGRAM ELEMENT NO.	PROJECT NO.	TASK NO.	WORK UNIT ACCESSION NO.

11. TITLE (Include Security Classification)
Report of Findings: Engineering Practices Study on Failure Analysis of NSN 5340-00-136-9872 Grooved Coupling Clamp

12. PERSONAL AUTHOR(S)
Hasiuk, Bohdan

13a. TYPE OF REPORT	13b. TIME COVERED	14. DATE OF REPORT (Year, Month, Day)	15. PAGE COUNT
Final	FROM _____ TO _____	88 Oct 3	32

16. SUPPLEMENTARY NOTATION

17.	COSATI CODES		18. SUBJECT TERMS (Continue on reverse if necessary and identify by block number)
FIELD	GROUP	SUB-GROUP	Clamp, Failure Analysis, Stainless Steel, Stress Corrosion, Fastenings
13	05		
11	06	01	

19. ABSTRACT (Continue on reverse if necessary and identify by block number)
Failure analysis of an aircraft exhaust pipe clamp indicated that the clamp material was significantly and seriously outside the specification requirements and that the clamp failed in stress corrosion mode. Non-compliance with the material requirements was the most important factor in the formation and subsequent propagation of stress corrosion cracks. Improved inspection requirements and consideration of a material with greater resistance to stress corrosion cracking are recommended.

20. DISTRIBUTION / AVAILABILITY OF ABSTRACT	21. ABSTRACT SECURITY CLASSIFICATION
☒ UNCLASSIFIED/UNLIMITED ☐ SAME AS RPT. ☐ DTIC USERS	Unclassified

22a. NAME OF RESPONSIBLE INDIVIDUAL	22b. TELEPHONE (Include Area Code)	22c. OFFICE SYMBOL
Bohdan Hasiuk	215-697-4518	DISC-ECM

DD FORM 1473, 84 MAR   83 APR edition may be used until exhausted.
All other editions are obsolete.

DEFENSE INDUSTRIAL SUPPLY CENTER
DIRECTORATE OF ENGINEERING AND STANDARDIZATION
DEPARTMENT OF DEFENSE STANDARDIZATION

REPORT OF FINDINGS
ENGINEERING PRACTICES STUDY
ON
FAILURE ANALYSIS
OF
NSN 5340-00-136-9872
GROOVED COUPLING CLAMP

PROJECT NO: 95GP-0301
DATE: 3 Oct 88

PREPARED BY: _Bohdan Hasiuk_
Bohdan Hasiuk
Metallurgist

APPROVED BY: _J. A. Quinn_
J. A. QUINN
Chief, Metals & Misc.
Hardware Branch

SUMMARY:

In September 1987 an in-flight failure of NSN 5340-00-136-9872 V-Band Clamp occurred in OH-58 Bell Helicopter.

As the result of this incident all the clamps of the operational OH-58 aircraft were removed and inspected and the aircraft were retrofitted with new clamps.

Since the original failed clamp was not available for failure analysis, AVSCOM supplied us with a failed (cracked) clamp removed from one of the OH-58 aircraft.

Using the facilities of SPS Technologies a failure analysis was performed on this clamp.

The failure analysis revealed that:

1. The clamp material was significantly and seriously outside the specification requirements.

2. The clamp failed in stress-corrosion mode.

3. The non-compliance with the clamp's specification requirements was the most important contributing factor to the formation and the subsequent propagation of stress-corrosion cracks.

INTRODUCTION:

In September 1987 an in-flight failure of NSN 5340-00-136-9872 V-Band Clamp occurred in OH-58 aircraft (1).

The clamp, called out on the National Utilities Corporation (NUCO) drawing 4606 AC, is made from CRES (corrosion resistant steel) material and supports the gas exhaust pipe of the OH-58 aircraft. National Utilities Corporation was contacted and we were informed that the CRES material was made to AMS 5595C specification requirements (2).

As the result of this incident all the clamps of the operational OH-58 aircraft were retrofitted with new clamps.

Since the original failed clamp was not available for failure analysis we asked AVSCOM to supply us with another clamp (which was removed from the aircraft and found to be cracked).

In due time we received a cracked clamp and, using the facilities of SPS Technologies, performed a failure analysis of the subject clamp.

1

VERIFICATION OF SPECIFICATION REQUIREMENTS

Since the National Utilities Corporation drawing 4606AC simply called out CRES (corrosion resistant steel) for the band material, we called National Utilities Corporation to find out the actual material from which the band was supposed to have been made. The Chief Engineer of NUCO (National Utilities Corporation) informed us that the band was made to AMS 5595C specification (2).

AMS 5595C specifies a nitrogen strengthened AISI 202 type of stainless steel with some significant chemical variations. AMS 5595C specifies that the material should be solution treated at 1950^c F $\pm$ 25" F and rapidly cooled. This heat treatment produces an, essentially, annealed material with considerable ductility. The specification calls out 40% minimum elongation (using 2 inch gauge length specimens), 60 ksi minimum yield strength and 100 ksi minimum tensile strength; the hardness is specified as 100 HRB maximum (equivalent to HRC 23). The grain size is specified as ASTM No 7 or finer (based on the 2^n formula). The specification also calls out a bend test and a "periodic" test for embrittlement (i.e., chromium-carbide precipitation at grain boundaries).

Because of the limited facilities at SPS Technologies and because of the material limitations (the band is 0.040 inches thick), only chemical analysis, grain size and hardness tests were performed on the band material. The results of these tests are shown in Tables I and II and in figures 1 through 1C.

Examining Tables I and II and figures 1 through 1C, the following generalizations can be made:

1. The band is ($\frac{0.21-0.04}{0.04}$) more than 400% above the maximum in carbon content. This is both significant and critical and will be discussed later in this report.

2. The slight deviations (from specification requirements) in nickel and chromium are insignificant.

3. A rather large ($\frac{32.5-23}{23}$ = 41%) deviation (of the band) in hardness, from the specification requirements, is troublesome and will be discussed in this report.

MICROSCOPIC AND FRACTOGRAPHIC EXAMINATIONS:

An isometric view of the clamp is shown in figure 2, while figure 2A shows the actual clamp at 0.40 magnification (reduction).

A section of the clamp containing the crack was cut out and is shown in figure 2B (with the arrow pointing to the crack). The area containing the crack is shown in more detail in figures 2C through 2E. Examining figures 2C through 2E, the following generalizations can be made:

2

1.   The main crack lies at about 45 degrees to the longitutinal (circumferential) direction of the clamp. This is important from the view point of the resolution of forces (stresses) acting on the clamp.

2.   More cracks were discovered in the vicinity of the rivet hole. All these cracks were at approximately 90 dgreees to one another and at approximately 45 degrees to the longitutinal (circumferential) direction. Furthermore, the new incipient cracks were on the outside surface and all of these cracks appear to have originated from the rivet hole.

In order to examine the fracture surface of the main crack (crack labeled "A" in figures 2D and 2E), a section of the clamp (containing the crack) was cut out and is shown in figures 3 through 3B.

Before the fracture surface was examined by the Scanning Electron Microscope, an EDS analysis was made of both the newly opened surface (SES laboratory) and the crack surface, and the results are shown in figures 4 and 4A.

Examining figure 4 it becomes obvious that we are looking at austenitic stainless steel (very strong primary and secondary iron lines as well as significant cnromium, nickel and silicon lines). However, when we look at figure 4A, which represents the EDS analysis of the crack surface, we see an extremely strong chloride line and very significant sulfide, potassium and sodium lines. This represents quite a "zoo" of corrodents with the most powerful corrodent, namely chloride, in extremely high concentrations.

Following the EDS study, the fracture surface of the main crack was examined by Scanning Electron Microscope and the significant/representative areas were photographed and the results are shown in figure 5 through 5C. Examining the fracture topography of this crack it becomes obvious that we are dealing with intergranular/transgranular fracture mode (a rather rare phenomenon in austenitic stainless steels). Furthermore, we see some evidence of secondary cracking on the fracture surface.

Because the surface of this crack was covered with corrosion products and in order to preclude any possibility of the incorrect interpretation of the fracture mode (i.e. interpreting "fractures" in the corrosion layer as a crack fracture) - the fracture surface was cleaned ultrasonically for one minute in inhibited HC1 solution. After the cleaning, the fracture surface was re-examined by SEM and the significant/representative areas (as close as possible to the original significant/representative areas) were photographed and the results are shown in figures 6 through 6D.

As a final step in the examination and evaluation of this fracture surface, the fracture was once more ultrasonically cleaned, this time for three minutes, in the solution of inhibited HCL. After the cleaning the fracture surface was re-examined and the representative/significant areas photographed. The results are shown in figures 7 through 7B.

3

Examining all the fractographs of the fracture surface the following statements can be made:

1.   The crack originated on the outside surface of the clamp at the rivet hole (underneath the rivet).

2.   The crack originated in an intergranular stress-corrosion mode.

3.   As the crack progressed the intergranular mode began to change to intergranular/transgranular mode with a slight corrosion fatigue component. The change in failure mode resulted from a change in crack propogation (i.e., the crack began to accelerate due to the reduction of load carrying area and the resultant increase in stress). The load carrying area (cross-section of the clamp) was continuously reduced not only because of the continuing propogation of the main crack but also because new cracks were forming.

DISCUSSION

Based on all the evidence presented heretofore we will attempt to reconstruct all the events which led to the failure (i.e. crack formation) of this clamp.

To begin with the clamp was seriously out of specification both in carbon content and in hardness.

It is a well known fact (3) that austenitic stainless steels, if cooled slowly through the temperature range of about 1500 degrees F to 1000 degrees F, will precipitate chromium carbides at grain boundaries thus depleting chromium from the close proximity of the grain boundaries and making the material extremely susceptible to intergranular stress corrosion cracking. This is the primary reason why in austenitic stainless steels (which are strenghtened by cold work and not by heat treatment) the carbon is kept to an absolute minimum (in the case of AMS 5595 it is specified as 0.04% maximum). All the evidence presented heretofore (very high carbon content, i.e. 0.21% vs.the specified maximum of 0.04% as well as the intergranular failure mode) points to sensitization (precipitation of chromium carbides at grain boundaries in the temperature range of about 1000 F to 1500 F) of the band material. This sensitization could have occured either during heat treatment (i.e., solution heat treatment paragraph 3.3 in AMS 5595) or in service. Since AMS 5595 specifies a rapid cooling through this temperature range we considered it prudent to investigate the possibility of sensitization during service.

Taking the geometry of the cross-section of the entire clamp under consideration, the metal temperature of the exahust pipe of the OH-58 helicopter would have to be considerably above 1000 F to cause the temperature of the outside clamp surface to reach 1000 F. This is graphically portrayed in figure 8.

4

After contacting Boeing-Vertol (4) and Bell Helicopter (5) (the manufacturer of OH-58 helicopter) - we were informed that the outside temperature of the exhaust pipe never exceeded 1000 F and reached 1000 F only on rare occasions. From the heat transfer considerations this would put the temperature of the outside surface of the clamp at about 600 to 700 degrees F maximum. We must conclude, therefore, that the sensitization of the clamp material occured during heat treatment! Furthermore, on our own initiative we asked the SPS to do a titanium/columbian analysis. Titanium and/or columbium is sometimes added to austenitic stainless steel for stabilization purposes (so that titanium and/or columbium will "tie up" the carbon and thus preclude it (carbon) from combining with chromium). SPS laboratory did, in fact, find 0.45% titanium in the band material, thus proving that NUCO (or the maker of the band material) was either aware of sensitization problem or was unsure of its ability to control carbon, or both (6).

The high carbon and the higher than specified hardness are necessary but not sufficient conditions for the corrosion component of the stress corrosion failure mode.

"Stress-corrosion cracking in austenitic stainless steels has been reported in chloride solutions when high stresses (residual or applied) are present in the metal" (7). "Sensitized material may display stress assisted intergranular corrosion having a cracklike appearance under conditions where intergranular attack in unstressed material would be minor (7). Crevices formed by joints and connections are most frequently subject to attack. In a crevice, the oxygen supply is limited and cannot repair the passive oxide film and a so-called "differential concentration cell appears". (7) "Intergranular stress-corrosion cracking occurs most often in polythionic acid (sulfur based) solutions." (7)

Since the crack originated under the rivet head (crevice attack) and large concertration of sulfur (polythionic acid) and chlorides were found (figure 4A) - all the corrosion conditions for stress corrosion cracking were present.

Having disposed of the corrosion component of the stress-corrosion problem, let us look at the stress aspect of this problem.

When the helicopter engine is turned on, the exhaust pipe becomes hot and begins to heat the clamp. From heat transfer considerations, the inside surface of the clamp band heats up first. A thermal gradient (between the inside surface and the outside surface) is set up causing the inside surface of the clamp band to be in compression and the outside surface to be in tension.

The thermal gradient could be very large (at the start of the cycle) and if the material lacks sufficient ductility (higher than specified hardness and sensitization certainly show this to be the case) the resultant stresses: thermal (experienced during the initial heating of the exhaust

5

pipe) and mechanical (stress associated with the possible vibration of the exhaust pipe) could approach the strength of the material, and make the material susceptible to corrosion attack. Figures 2D and 2E suggest that this is precisely what happened.

As the tail pipe heated up, the clamp band began to experience thermal tensile stresses, (superimposed on the normal mechanical tensile/bending stresses) as was stated heretofore: the outside surface of the clamp was in (thermal) tension and the inside surface in (thermal) compression. Because of the clamp band geometry a two dimensional (plane stress) state of stress can be applied to this situation (8). The normal stresses in this state of stress are maximum in the longitutinal (circumferential) direction and minimum (in this situation close to zero) in the transverse (90 degrees to the longitudinal) direction. In such a state of stress the maximum shear stress will be at 45 degrees to the maximum normal stress. This is graphically portrayed in figure 9.

Looking at figure 9, the following conclusions can be made:

1. The maximum and minimum values of normal stress occur when the shear stress is zero.

2. The maximum and minimum values of both normal stress and shear stress occur at angles which are 90 degrees apart.

3. The maximum shear stress occurs at an angle halfway between the maximum and minimum normal stress.

Taking under consideration the fact that failure occurs at the maximum shear stress locations - figures 2D and 2E, which represent the crack formations in the clamp band, substantiate totally the above stress field analysis.

Figures 2D and 2E which portray crack formation 90 degrees to each other and 45 degrees to the maximum normal stress can also be explained by the application of the idealized single crystal Schmid's law (9):

$$\vec{\tau} = S \cos \lambda \cos \phi$$
   where:
$\vec{\tau}$ = shear stress
S = normal stress
λ = angle between the normal stress and the shear plane
ϕ = angle that a perpendicular to the shear plane makes with the direction of the normal stress

In this situation shear stress $\vec{\tau}$ is at a maximum when both λ and ϕ are 45 degrees.

Summarizing the discussion of this failure we see that <u>all</u> the conditions necessary for the formation and propagation of stress-corrosion cracks in the V Band Clamp were, indeed, present.
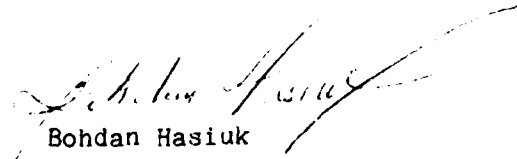
CONCLUSIONS

Based on the test results the following conclusions are made:

1. The NSN 5340-00-136-9872 grooved coupling clamp failed due to the formation of stress-corrosion cracks.

2. The crack topography indicates that the crack/cracks originated in the intergranular mode and propagated in the intergranular/transgranular modes.

3. The clamp material was significantly and seriously outside the AMS 5595C requirements:

   a. The carbon content was 400% above the maximum allowable, while

   b. The hardness was 41% above the maximum allowable

4. It is our belief that the high carbon sensitized the material while higher than specified hardness reduced the materials ability to redistribute stress (i.e. reduced the materials ductility).

5. The material's sensitization and its high hardness in association with the normal design stresses caused the formation and the subsequent proprogation of stress - corrosion cracks.

6. It is concluded, therefore, that the non-compliance with the AMS 5595C specification was a primary cause of this failure.

Recommandations

It is recommended that:

1. The inspection procedure to determine the compliance of the clamp bands with the AMS 5595C specification requirements ought to be reevaluated.

2. A serious attempt ought to be made to replace the AMS 5595 material (an AISI 202 type of stainless steel) with a material more resistant to stress corrosion cracking. An iron-base or a nicket base super alloy might be considered. A-286 (UNS K66286), Inconel 718 or Incoloy 925 certainly deserve consideration.

3. Since this type of clamp is subject to high stress excursions (both mechanical and thermal) and since it operates in corrosive environment, regular and thorough inspections (both visual and dye penetrant) are absolutely mandatory.

Bohdan Hasiuk

REFERENCES

1. Diers, Eleanor, "Conversation Record with Captain W. Servay of AVSCOM on the subject of Coupling Clamp NSN 5340-00-136-9872," 9 September 1987, 9:30 A.M.

2. Hasiuk, B. "Communications with National Utilities Corporation Chief Engineer, Mr. George Yamamoto", 26 January 1988.

3. American Society of Metals, Failure Analysis and Prevention, Metals Handbook, Ninth Edition, Volume 11, pages 215-216.

4. Hasiuk, B. "Communications with Boeing-Vertol Corporation, Propulsion Technology Engineer, Mr. David Woodley", 8 August 1988.

5. Hasiuk, B. "Communications with Bell Helicopter Corporation, Power Plant Installation Engineer, Mr. Scott Horn," Forth Worth, Texas, 8 August 1988.

6. Hakun, Eric G., "Failed V-Groove Clamp", SPS Laboratories Test Report to B. Hasiuk, 27 January 1988.

7. American Society of Metals; Properties and Selection: Stainless Steels, Tool Materials and Special-Purpose Metals, Metals Handbook, Ninth Edition, Volume 3, pages 62-63.

8. Dieter, George E. Jr., "State of Stress in Two Dimensions (Plane Stress);" Stress and Strain Relationships for Elastic Behavior, Mechanical Metallurgy McGraw-Hill 1961, pages 19-23.

9. VanVlack Lawrence H., "Plastic Deformation within Single Crystals", Elements of Materials Science and Engineering, Fifth Edition, Addision-Wesley; 1985, pages 167-168.

TABLE I

CHEMICAL ANALYSIS, %

	C	Mn	Si	P	S	Cr	Ni	N	Mo	Cu
Failed Band :	0.21	10.00	0.74	0.015	0.006	18.97	7.52	(1)	0.43	0.41
AMS 5595C, Min. :	-	8.00	-	-	-	19.00	5.50	0.15	-	-
Requirements, Max:	0.04	10.00	1.00	0.060	0.030	21.50	7.50	0.40	0.75	0.75

TABLE II

TENSILE AND HARDNESS RESULTS

	Tensile Strength, ksi	Yield Strength, ksi	Elongation, %	Hardness HRC(2)
Failed Band :	(3)	(3)	(3)	32.5 (4)
AMS 5595C, Min. :	100	60	40	23 (5)
Requirements, Max.:	-	-	-	-

Notes: 1 = SPS Technologies have no means of measuring Nitrogen in steel
2 = Converted from HRB
3 = Because of material limitations, it was not possible to perform the tensile test
4 = Converted from Rockwell Superficial 30N reading of 52.7
5 = Converted from AMS 5595C requirement of 100 HRB
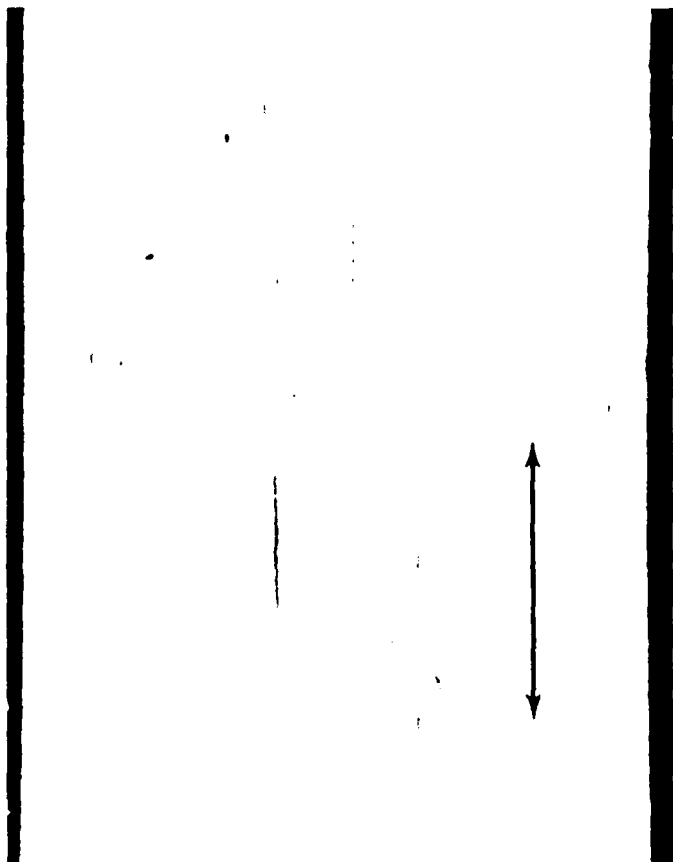
Figure 1 - 100X.   Unetched
photomicrograph of the clamp
material in the longitudinal
(circumferential) direction.
Note the highly elongated
stringers (probably sulfides)
suggesting longitudinal rolling.
The superimposed doublepoint
arrow shows the longitudinal
direction.
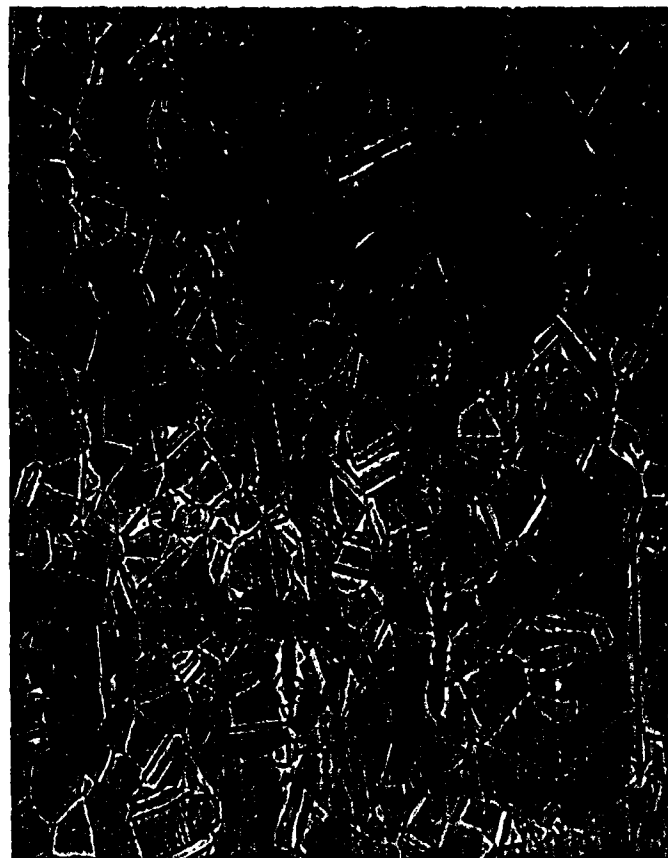
Figure 1A - 500X.   Same as figure 1,
only etched and at higher magnification.
Note the presence of the elongated
non-metallic stringers.   The long-
itudinal (circumferential) direction
is indicated by a superimposed
arrow.

Figure 1B - 100X. Photomicrograph showing the general microstructure in the transverse (cross-section) direction.
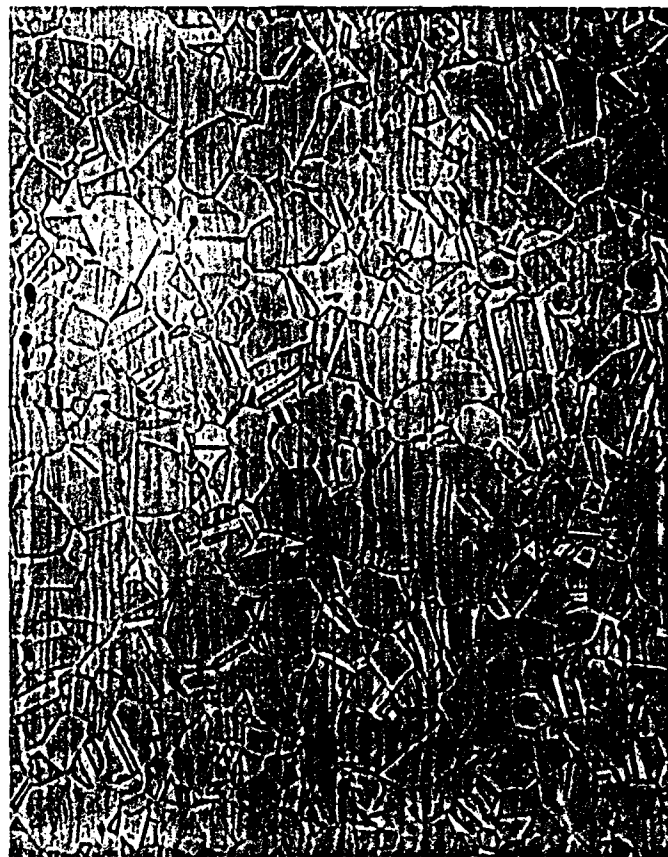
Figure 1C - 500X. Same as figure 1B, only higher magnification. Note the spherical shape of the non-metallic inclusions (probably cross-sections of the stringers from figures 1 and 1A).
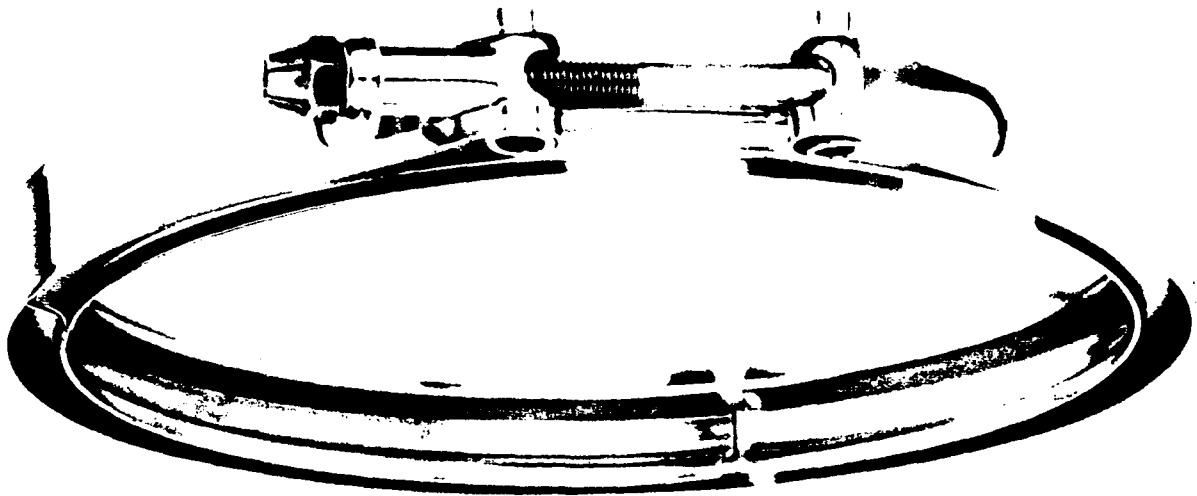
Figure 2. An isometric of the NSN 5340-00-136-9872 V-Band Coupling Clamp
made by National Utilities Corporation to Dwg: 4606AC.
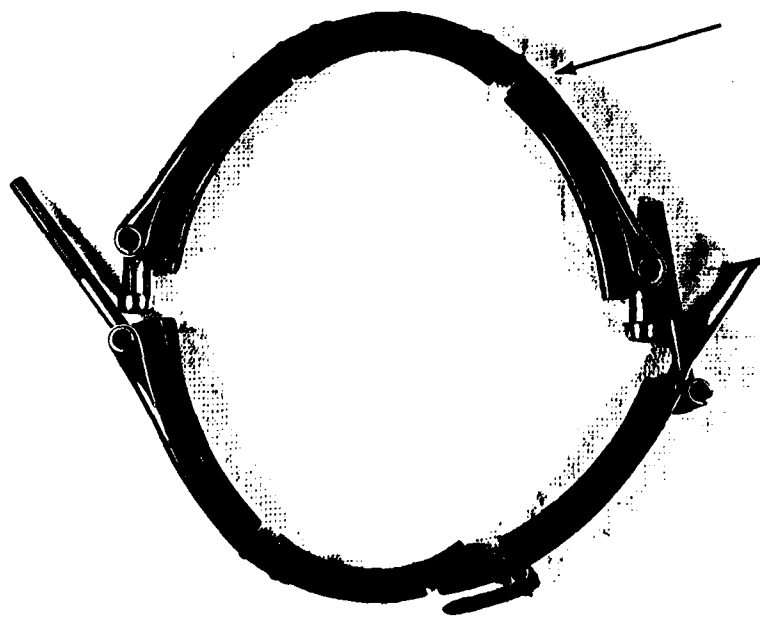
Figure 2A - 0.4X. The as-received V-Band coupling clamp.
The arrow indicates the rivet area of the clamp where a
crack was found. The area of the crack is shown in more
detail in figure 2B.
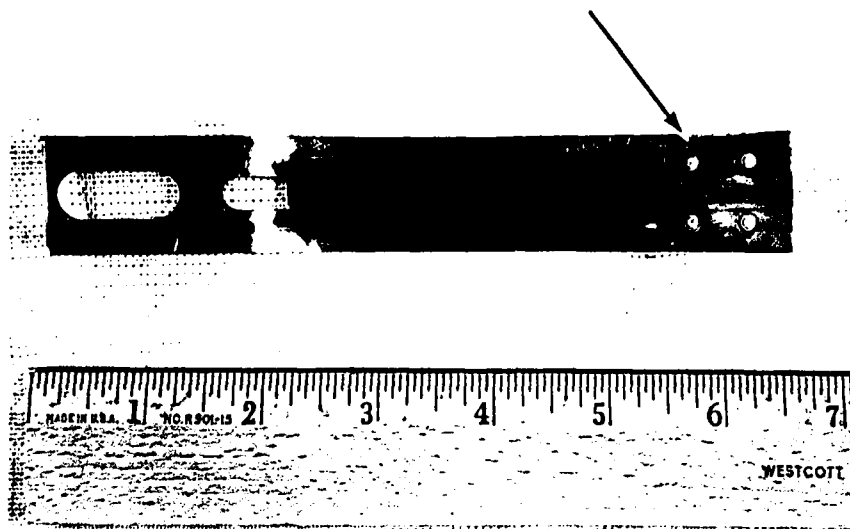
Figure 2B - 0.63X. Inside surface of the clamp showing the four rivet holes. The arrow points to a crack in the close proximity to one of the rivet holes. The area indicated by the arrow is shown in more detail in figure 2C.
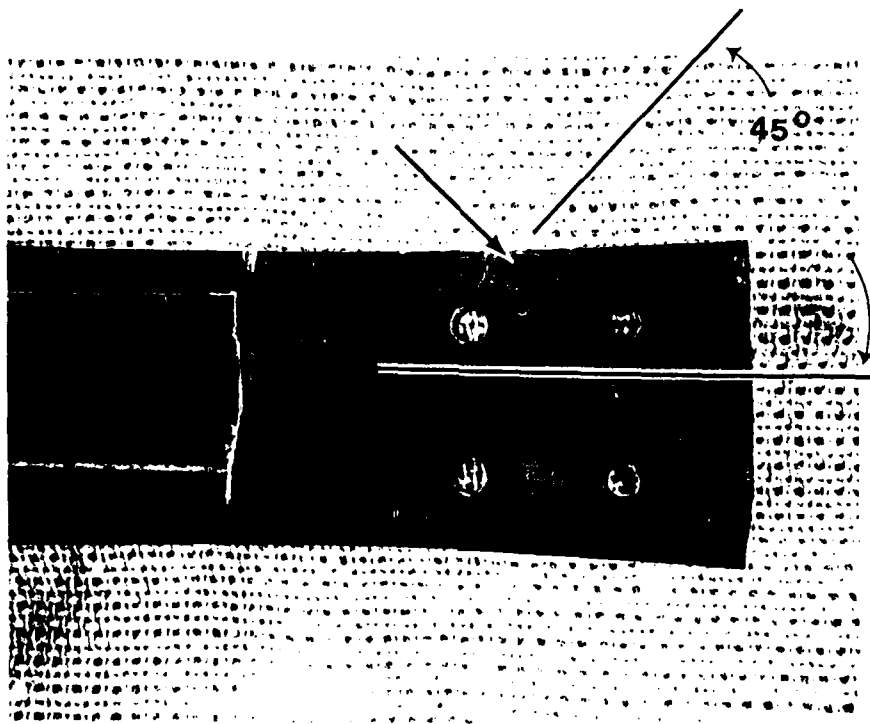
Figure 2C - 1.5X. A more detailed view of the inside
surface of the clamp from figure 2B. The arrow points
to a crack, which is plainly visible. Note that the
crack is at approximately 45° to the circumferential
direction (of the clamp). This area is shown in more
detail in figure 2D.
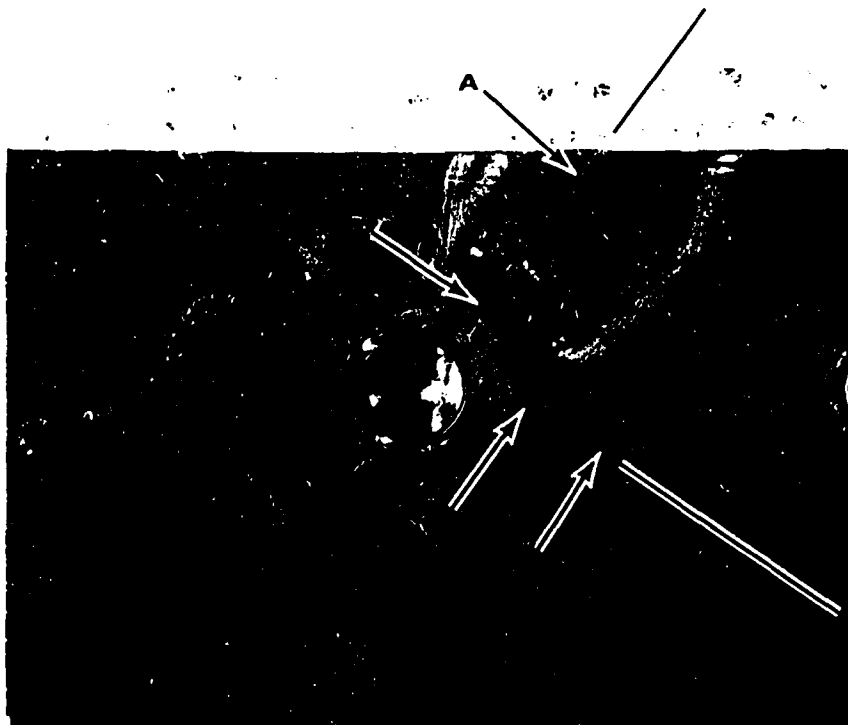
Figure 2D - 4.25X. Inside surface area of the clamp from figure 2C. Arrows labeled "A" indicate the main crack, while arrows labeled "B" show a small incipient crack. Note that this small incipient crack is normal (90°) to the main crack (both cracks are at 45° to the longitudinal (circumferential) direction. Note that neither the main crack nor the small secondary crack actually emanate from the rivet hole. The reverse (outside) area of this rivet hole (and the surrounding clamp material) is shown in figure 2E.
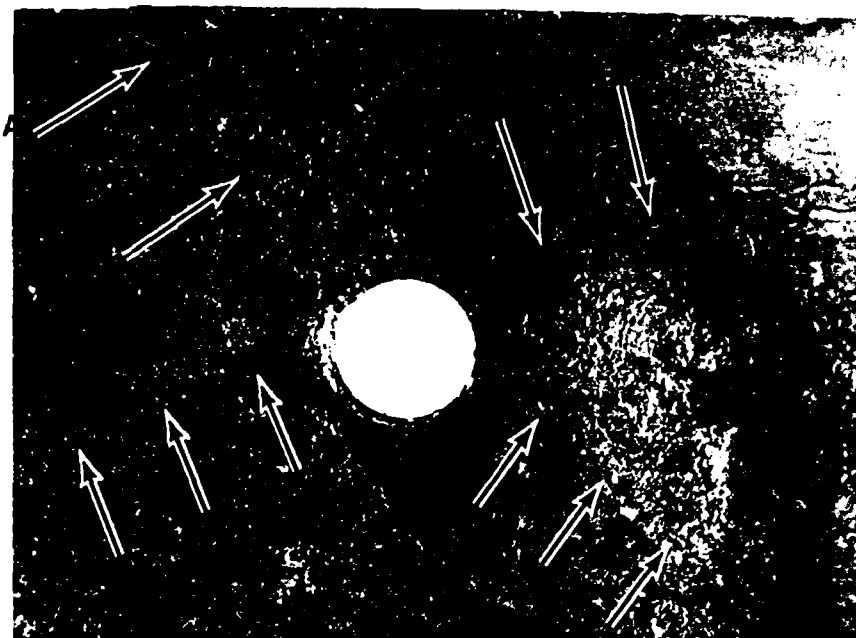
Figure 2E - 6X. Same area as the one shown in figure 2D - only this is the
outside (reverse) surface of the clamp. Arrows "A" point to the main crack;
arrows "B" point to a small incipient crack (identified as "B" in figure
2D); while arrows "C" and "D" identify two areas where cracks are forming.
Note that all cracks are at approximately 90° to one another and at
approximately 45° to the circumferential (longitudinal) direction of the
clamp. Also note that all four cracks actually emanate from the rivet hole.
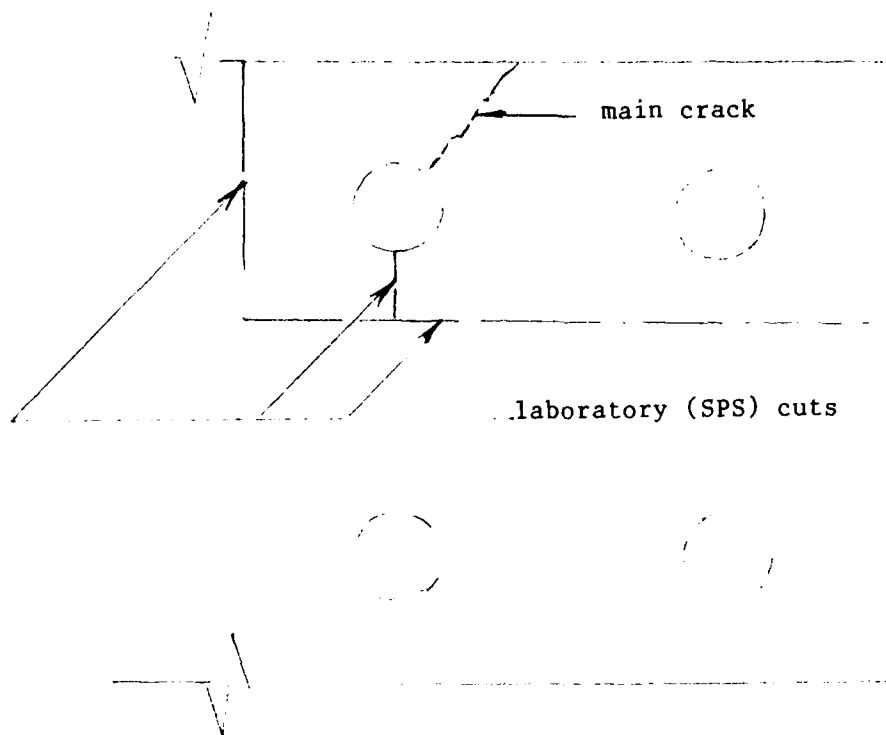
Figure 3-3.25X. A sketch of the inside surface of the clamp segment from figures 2B and 2C containing the crack. A part of this clamp segment was cut out and the crack was opened and is shown in figures 3A and 3B.

Fracture (crack) surface

Outside clamp surface → ← —·—·— Inside clamp surface

Rivet hole

Laboratory (SPS) cut
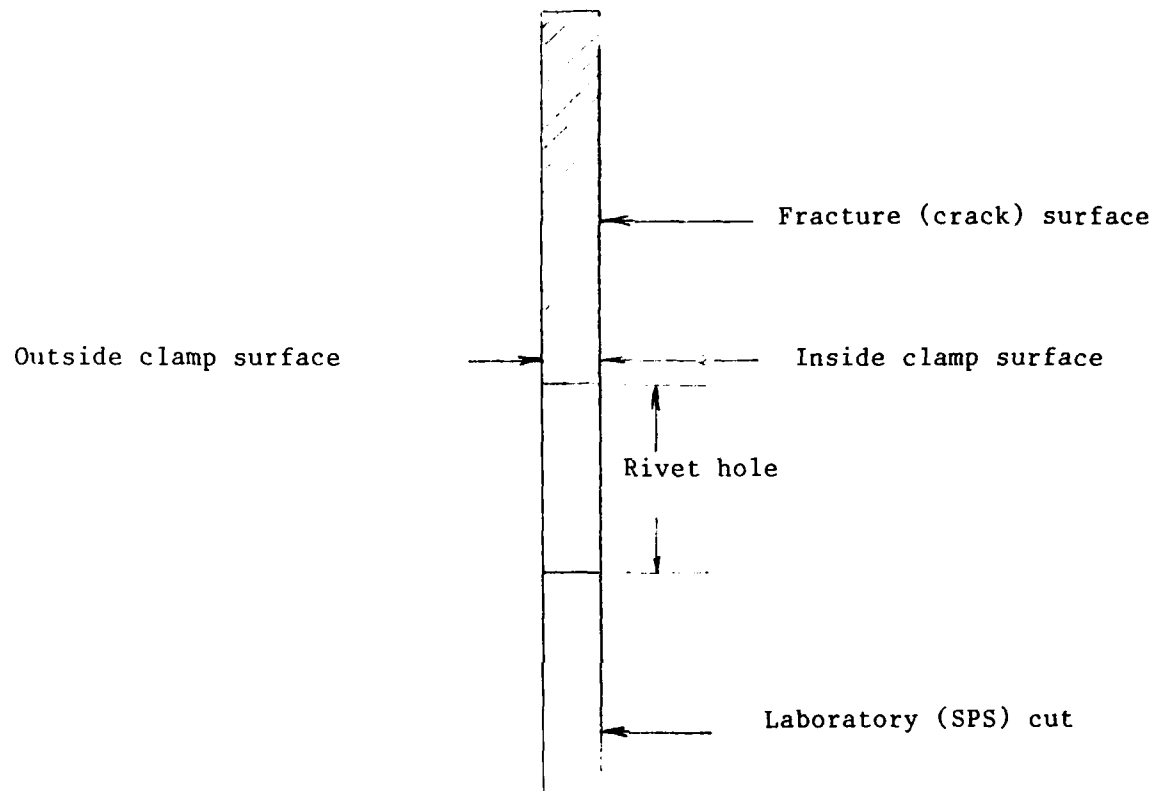
Figure 3A-9.75X - A sketch, from figure 3, of the opened main
crack and its relation to the clamp segment. A more detailed
sketch of the crack surface is shown in figure 3B.

Edge of the clamp

④

Outside of the clamp

Direction of crack propagation

③

Crack surface

Inside surface of the clamp

Direction of crack
propagation

Broken in the SPS
laboratory - tensile
overload.

②

①

Crack origin

Rivet hole
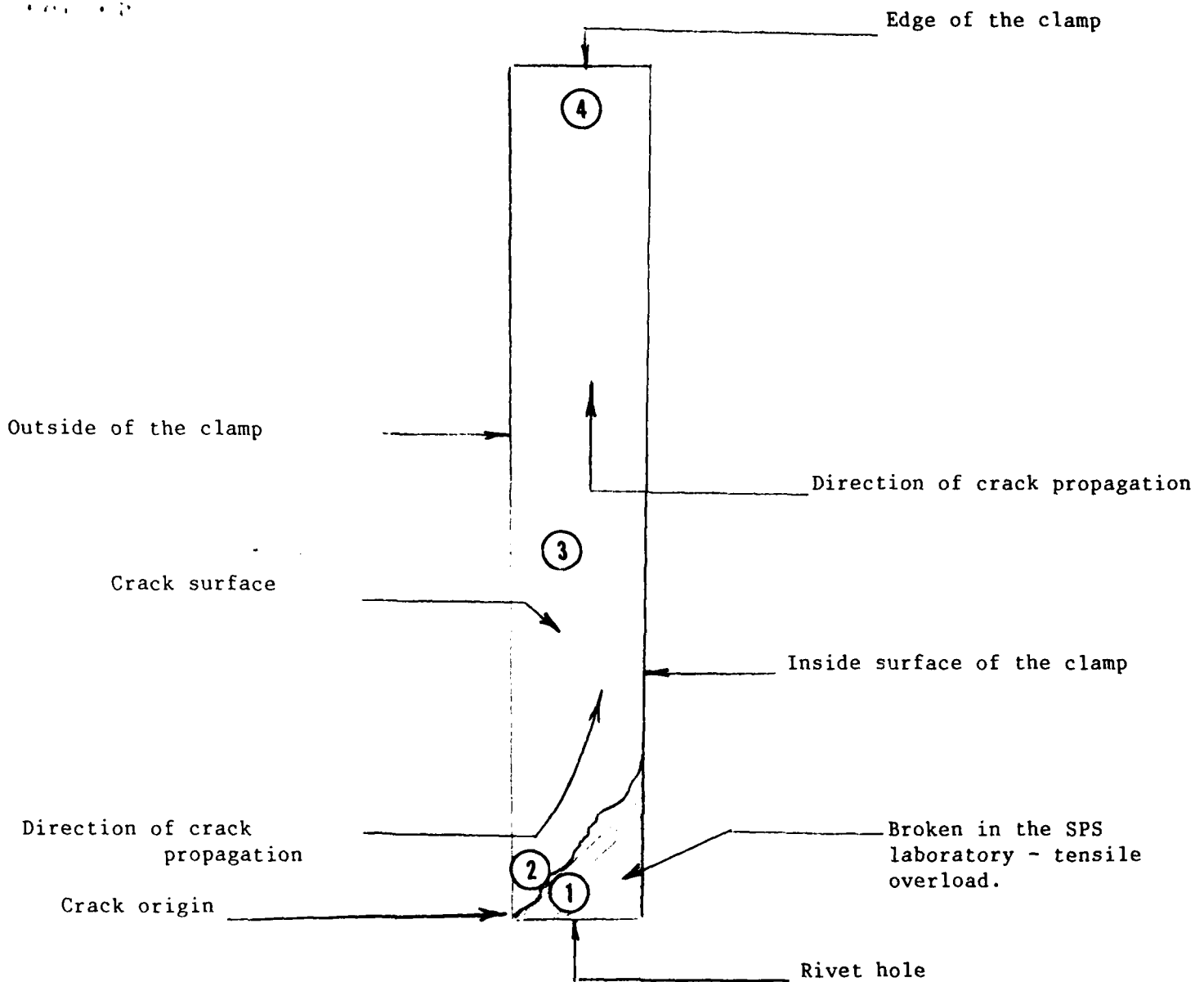
Figure 3B-20X. A sketch of the crack surface from figure 3A. The
surface of this crack was examined by the Scanning Electron
microscope (SEM) and was analyzed by Energy Dispersive Spectroscopy
(EDS) and the representative areas (labeled 1 through 4 in this
sketch) were photographed and the results are shown in figures
4 through 5A.
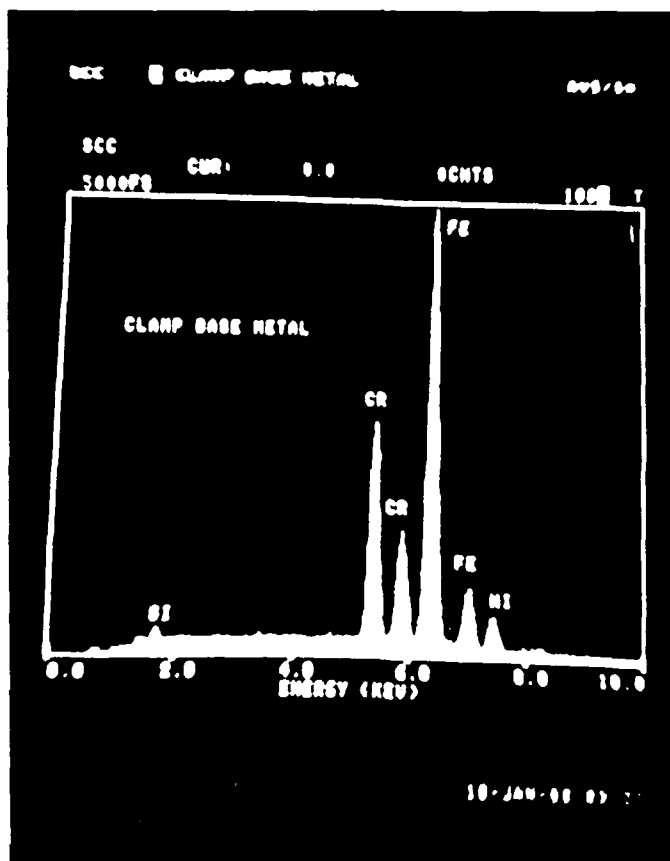
Figure 4. Energy Dispersive Spectroscopy (EDS) of the clean (broken in the laboratory) surface showing the basic chemistry of the clamp material (AMS 5595, iron-chromium-nickel alloy).
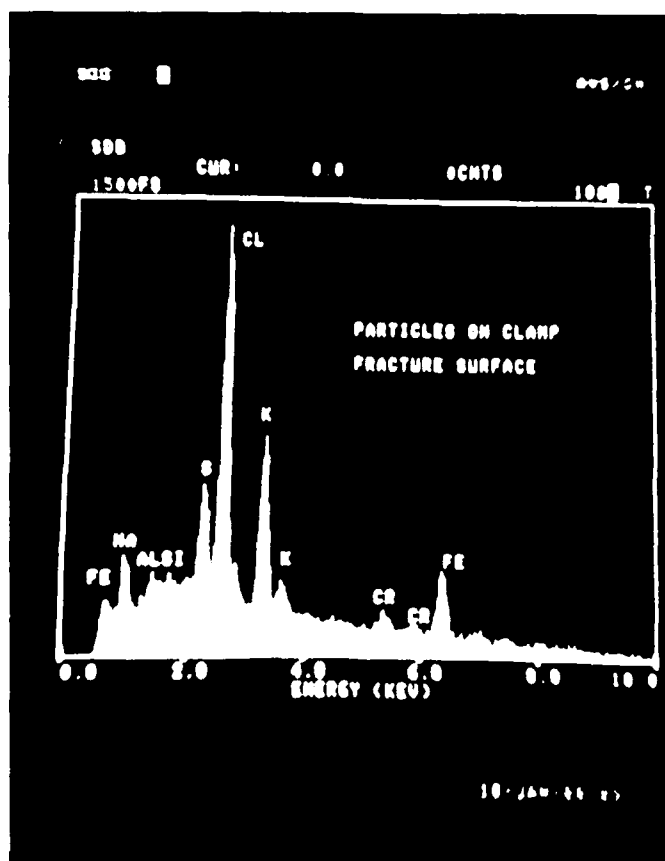
Figure 4A. Energy Dispersive Spectroscopy (EDS) of the particles found on the surface of the opened crack ("A" crack of figures 2D and 2E). Note the relatively high concentrations of chlorides and sulfides.
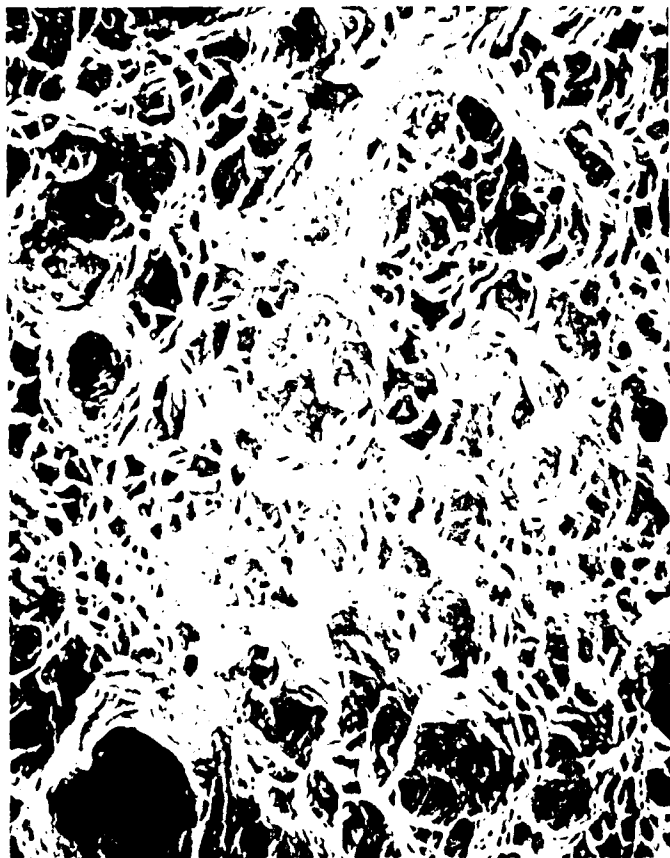
Figure 5 - 1900X. Area "1" from figure 3B showing a typical overstressed (tensile) "dimple" topography. This is a fracture produced by SPS Laboratory in the process of opening the main crack.
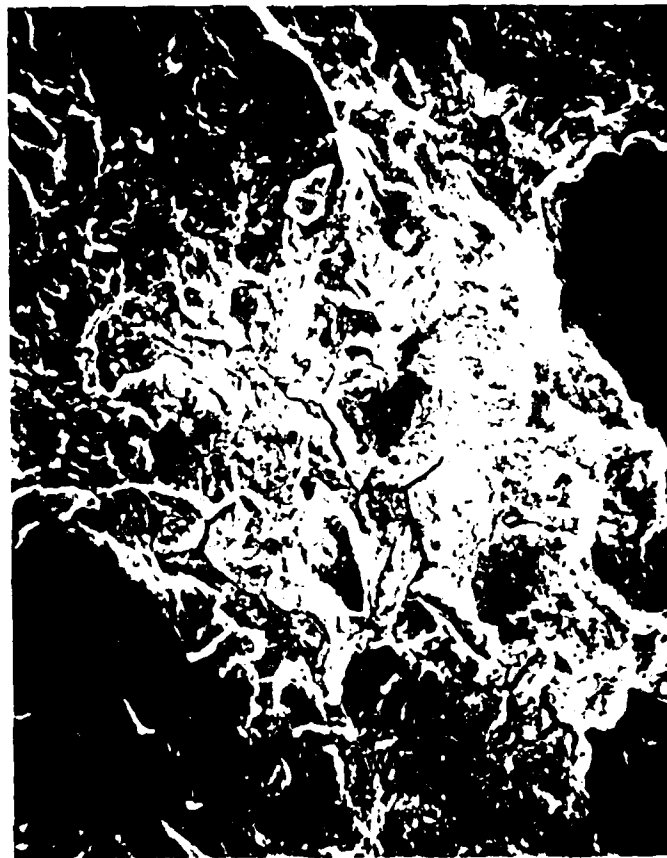
Figure 5A - 1900X. Fracture surface of the crack close to the origin of the crack, i.e. area "2" from figure 3B. Note the intergranular nature of the fracture topography (mixed with transgranular topography) and also note the presence of secondary cracks. Lower left hand corner of the fractograph shows smeared metal, suggesting some rubbing of the two crack surfaces.
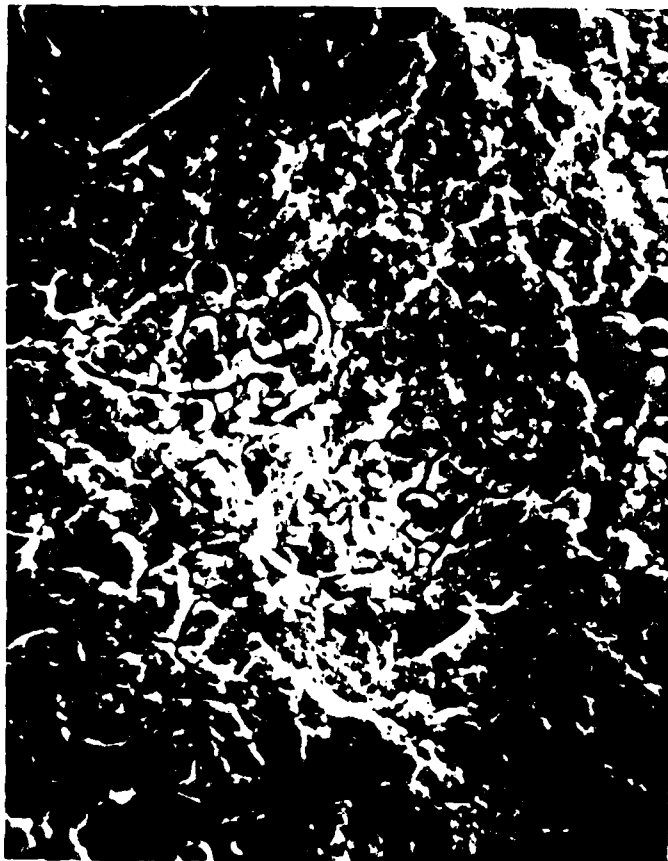
Figure 5B — 1400X. Area "3" (middle of the crack) from figure 3B. Again the intergranular nature of the crack topography is obvious (even though the fracture surface is obscured somewhat by corrosion products).
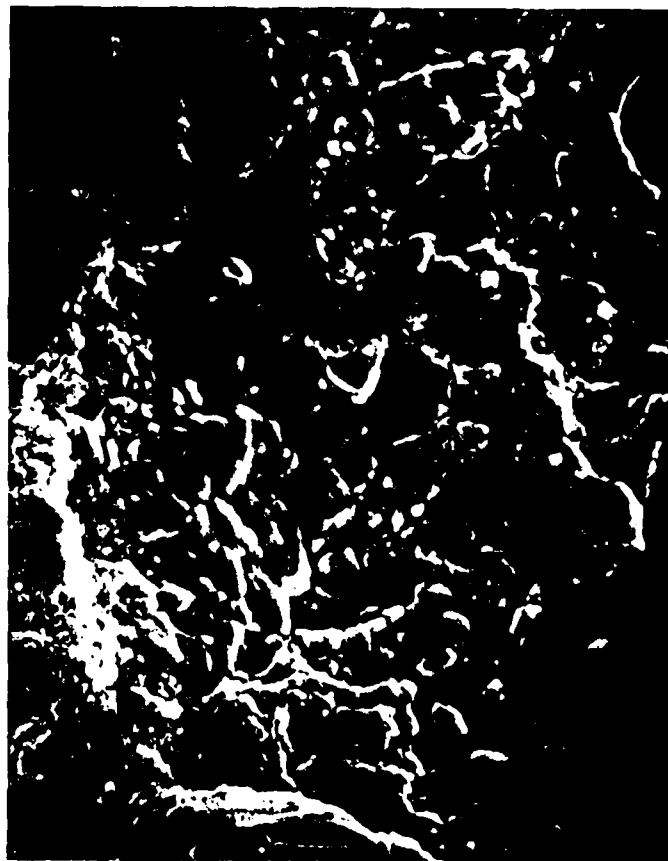
Figure 5C — 2000X. Area 4 (end of crack) from figure 3B. The topography is intergranular/transgranular with some evidence of secondary cracking.
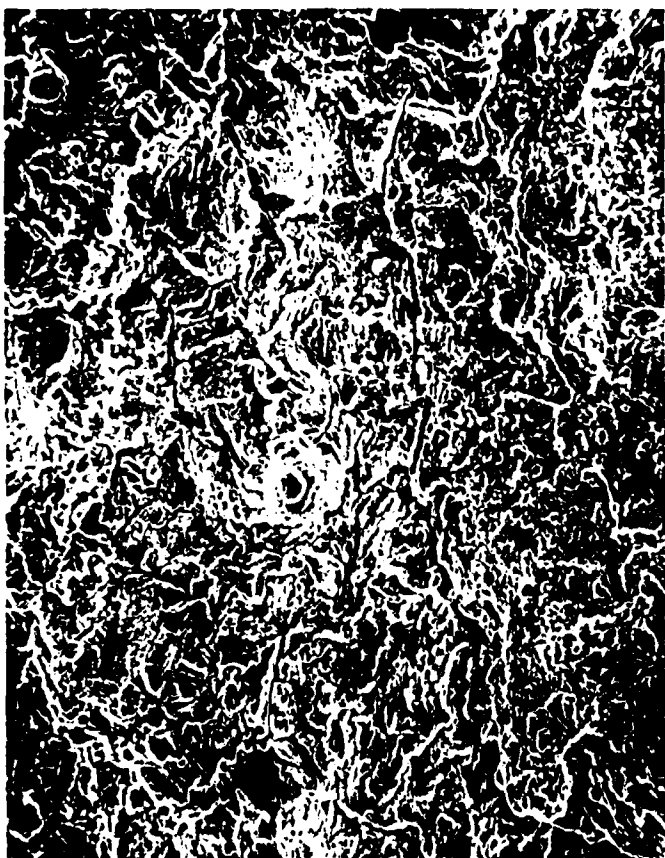
Figure 6 - 810X. Area "2" (near the crack origin) from figure 3B, <u>after</u> the fracture surface was ultrasonically cleaned in inhibited HCl. Note the intergranular/ transgranular topography and also note the presence of secondary cracks.
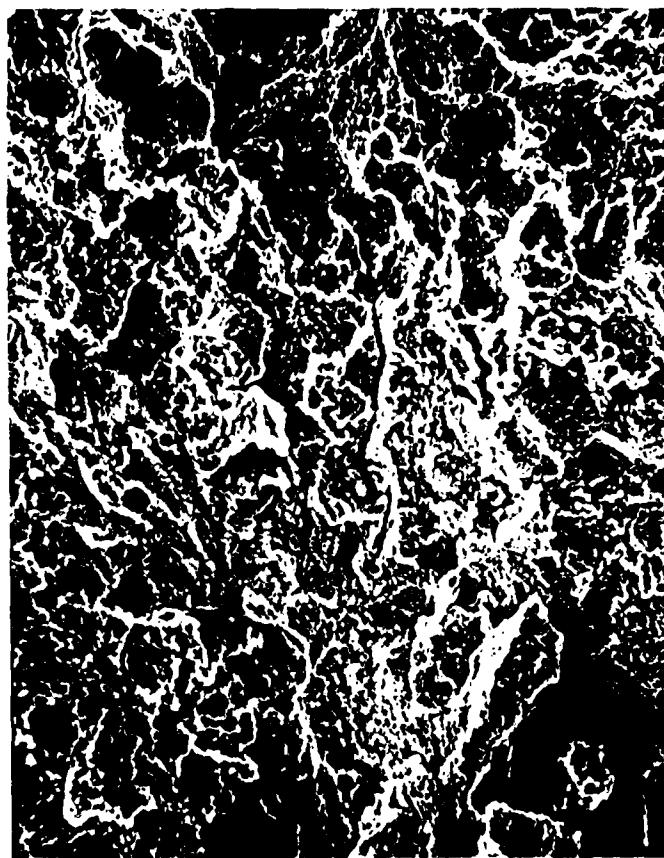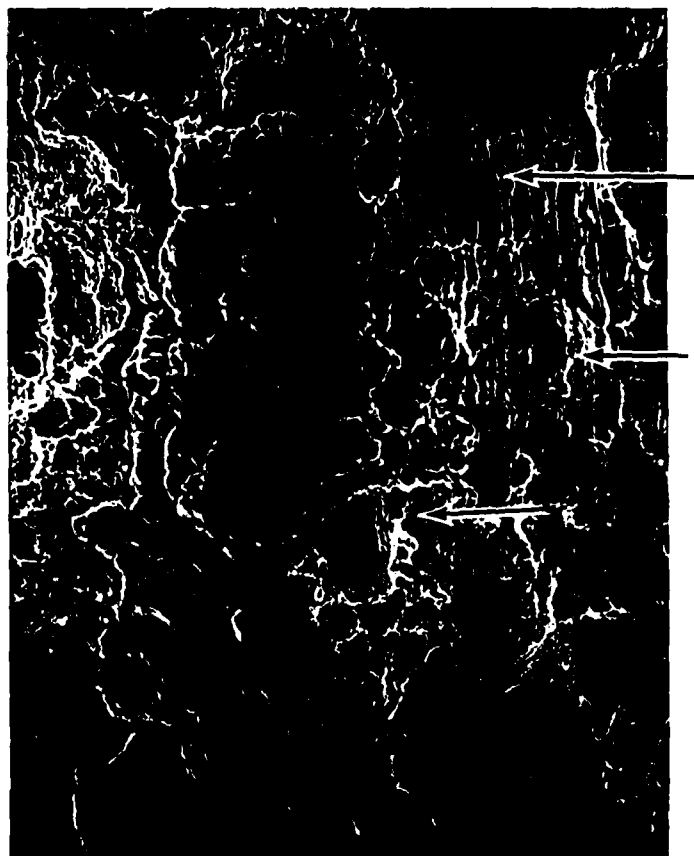
Figure 6A - 1900X. Area "3" from figure 3B after the fracture surface was ultrasonically cleaned in inhibited HCl solution. Note the intergranular (with some transgranularity) fracture mode.
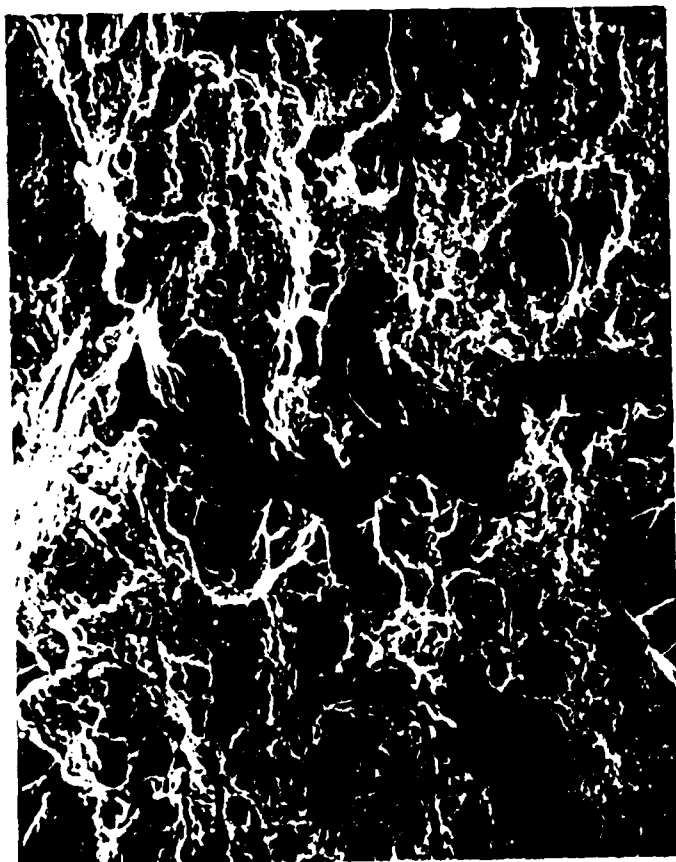
Figure 6B - 1900X. Area "3" from figure 3B after the fracture surface was ultrasonically cleaned for one minute in the inhibited HCl solution. Note the presence of secondary cracking.

Figure 6C - 1900X. Area "3" from figure 3B after the fracture surface was ultrasonically cleaned for one minute in the inhibited HCl solution. Note evidence of intergranular topography and also note some evidence of fatigue (indicated by the arrows). The fatique striations appear to be about 3×10^{-5} in. ($\sim 1/16"$ x 1/1900) in size.
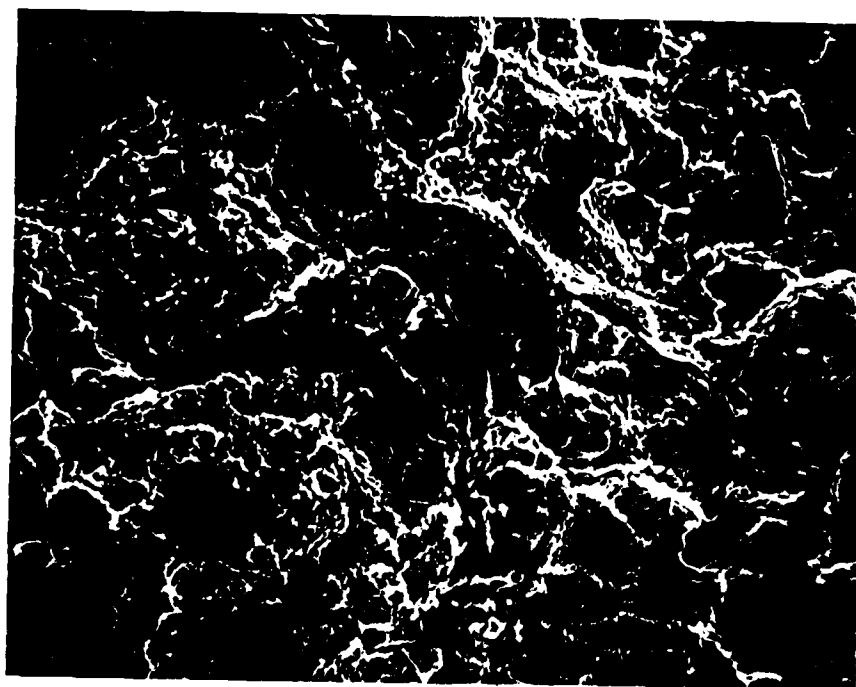
Figure 6D - 1900X. Area "4" from figure 3B after the fracture
surface was cleaned for one minute in inhibited HCl solution.
The fracture topography is intergranular/transgranular with
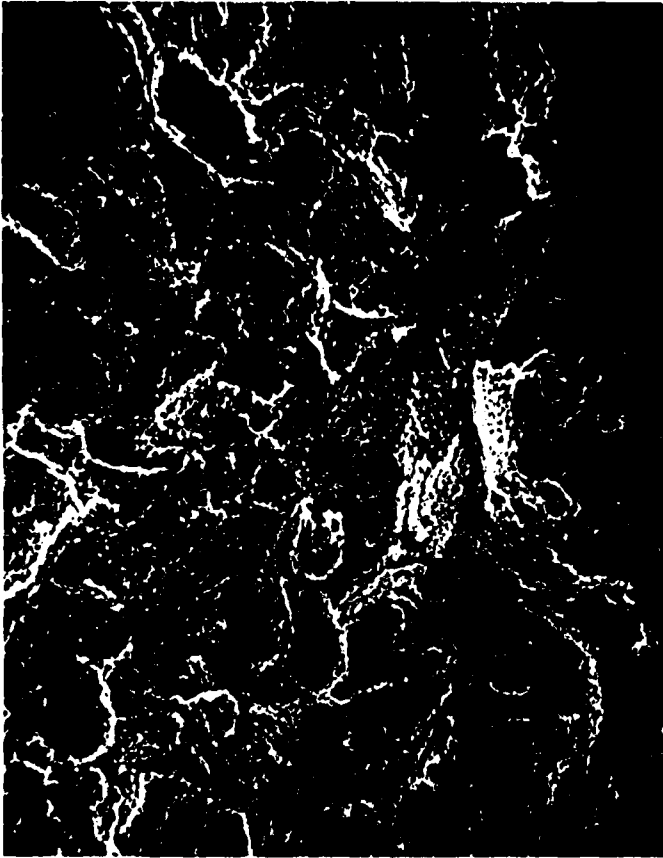evidence of secondary cracking.

Figure 7 - 1900X. Area "2" from figure 3B after the fracture surface was cleaned for three minutes (plus the previous one minute cleaning)in inhibited HCl solution. Note the obvious intergranular fracture mode. The pits on the fracture surface are, probably, the results of HCl cleaning.
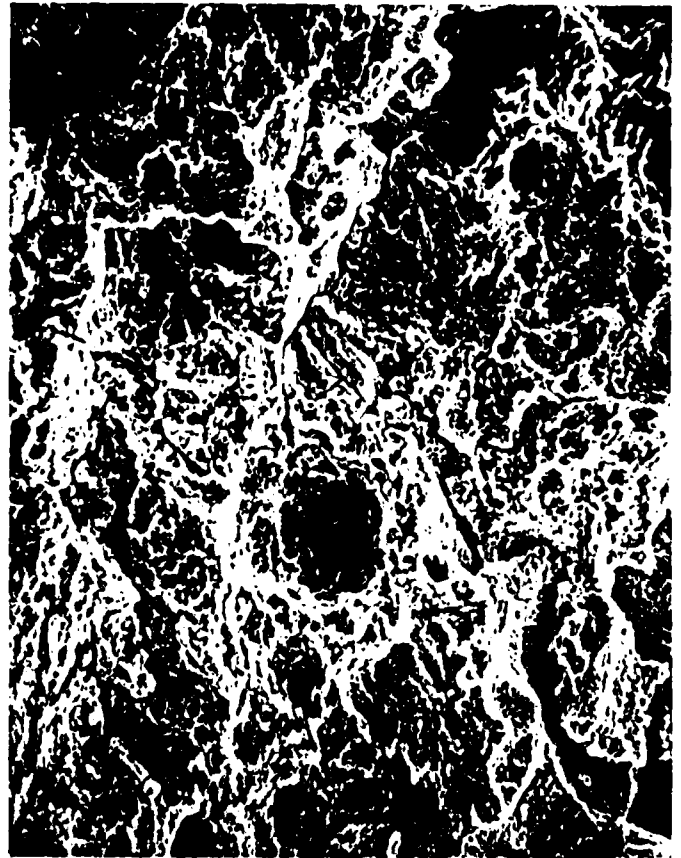
Figure 7A - 1900X. Area "3" from figure 3B after the fracture surface was cleaned for three minutes (plus the previous one minute cleaning) in inhibited HCl solution. The topography is intergranular/transgranular.
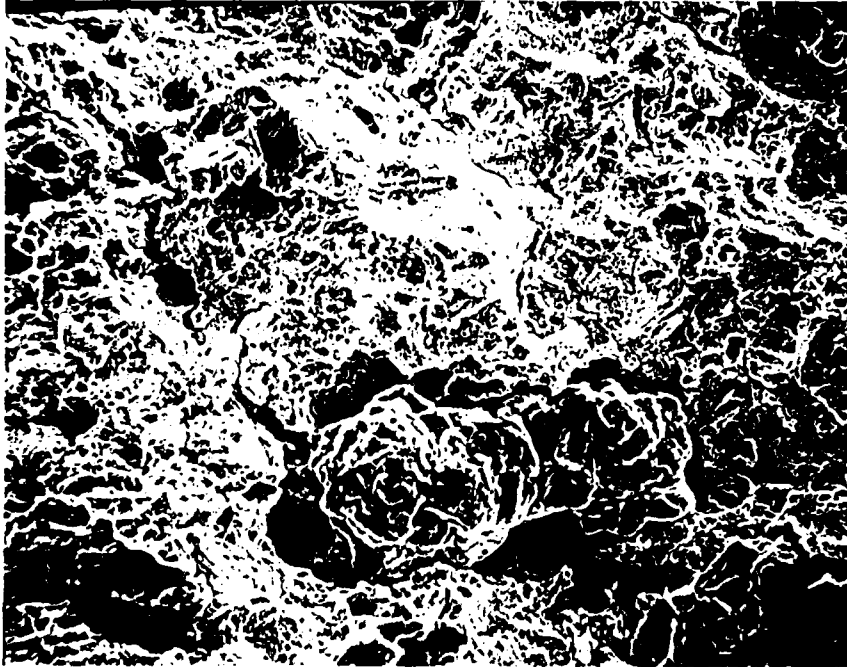
Figure 7B - 810X. Area "4" from figure 3B after the
fracture surface was cleaned for three minutes (plus
the previous one minute cleaning) in inhibited HCl
solution. Note that the topography is intergranular/
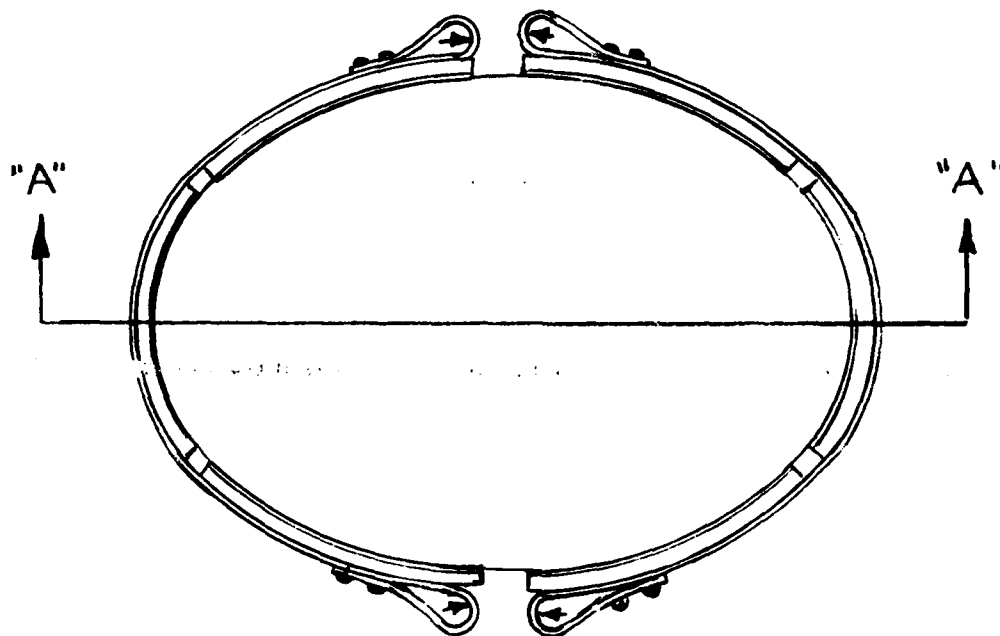transgranular and also note evidence of secondary
cracking.

Figure 8-0.55X. A sketch of the coupling clamp (which holds the exhaust pipe of the OH-58 helicopter). Section "A-A' is shown in figure 8A.

Outside band of the coupling clamp
(where the cracks were found)
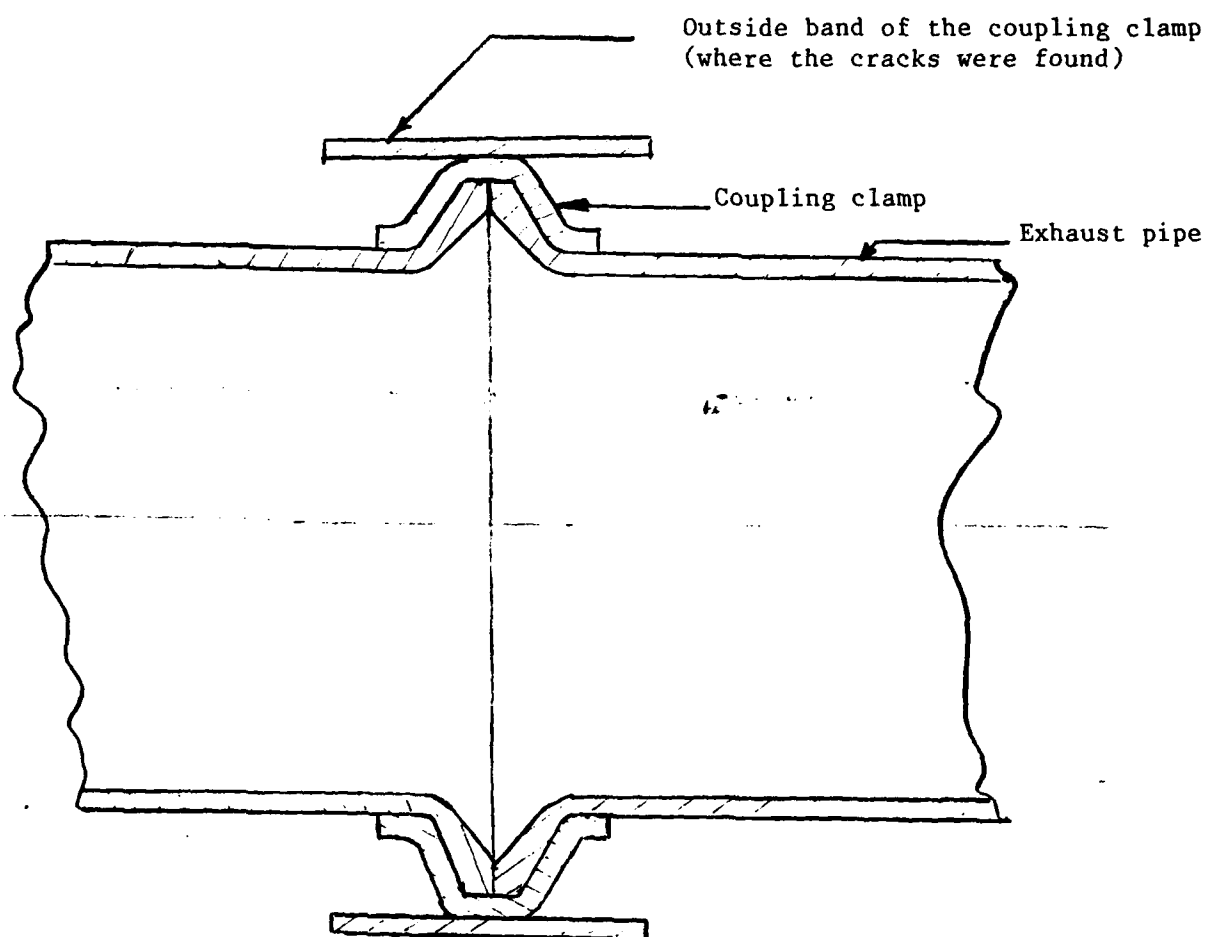
Coupling clamp

Exhaust pipe

Figure 8A - 0.44X.   Section "A-A" from figure 8 showing
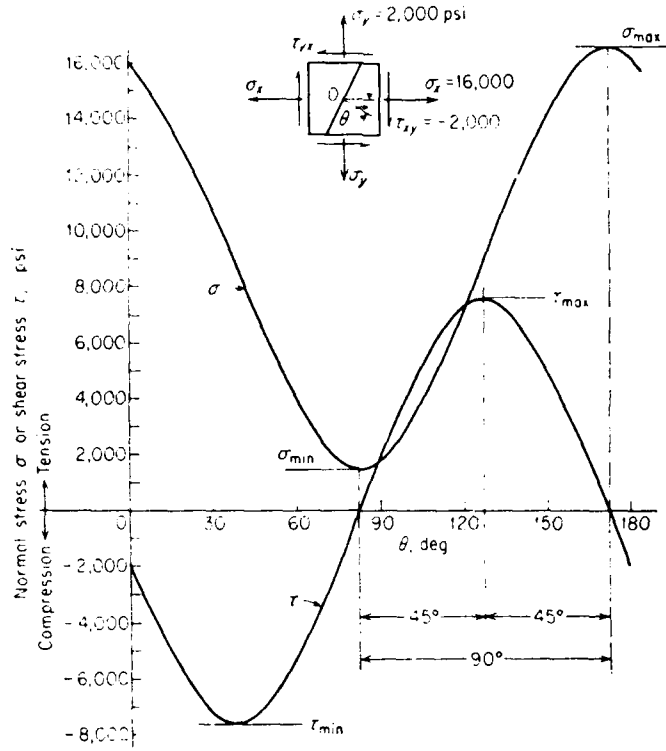the cross-section of the coupling clamp and the exhaust
pipe of the OH-58 aircraft.

Figure 9. Variation of normal (tensile) stress σ with
shear stress τ. The shear stress is at a maximum 45° away
from the maximum normal (tensile) stress. (Dieter, George E. Jr.
<u>mechanical metallurgy</u>, p. 21)